UCID- 17356

Lawrence Livermore Laboratory

Calculation of the Small Scale Self-Focusing Ripple Gain Spectrum For the CYCLOPS Laser System: A Status Report

J. A. Fleck, Jr., J. R. Morris, and P. F. Thompson

October 1976

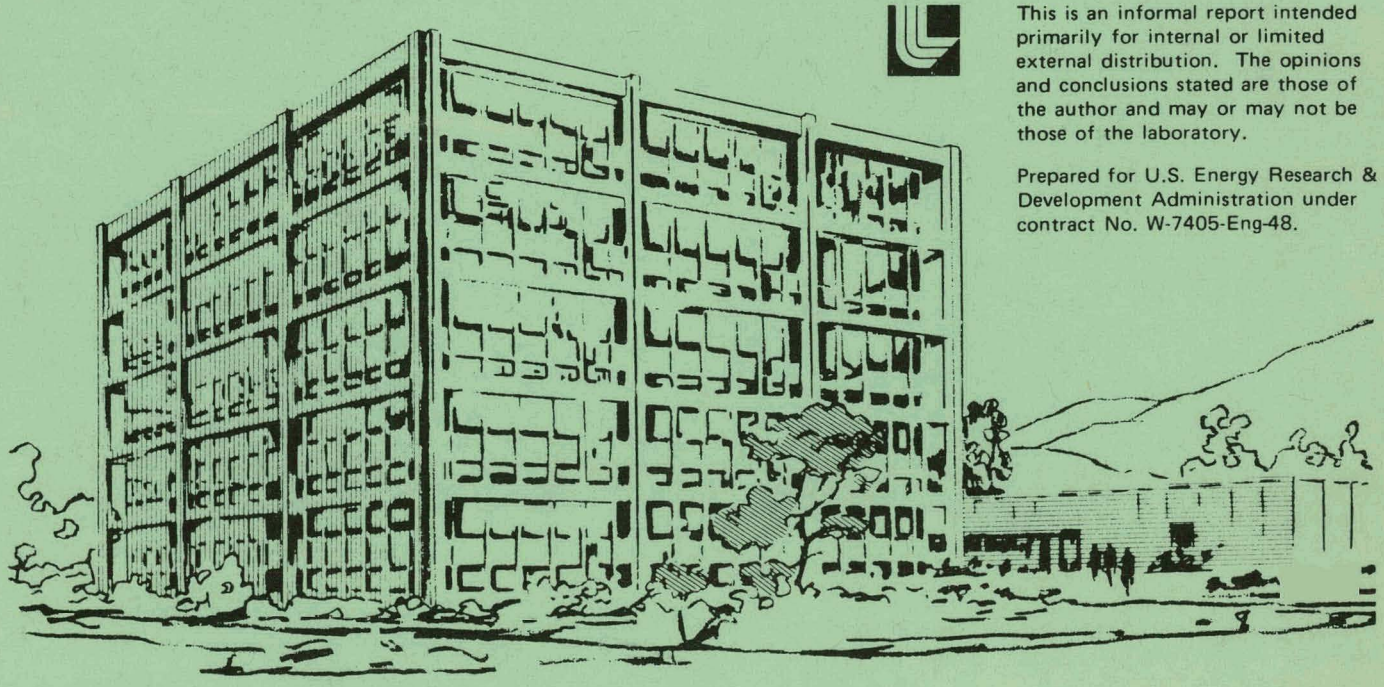

Prepared for U.S. Energy Research & Development Administration under contract No. W-7405-Eng-48.

DISCLAIMER

Calculation of the Small Scale Self-Focusing Ripple Gain Spectrum for the CYCLOPS Laser System: A Status Report

J. A. Fleck, Jr., J. R. Morris, and P. F. Thompson

Introduction

As is well known, nonlinear self-focusing can lead to beam deterioration or even beam breakup by amplifying small scale imperfections in the laser beam. This phenomenon can, of course, lead to a limitation in the maximum useful laser power. A simple linearized theory of this effect, valid for a single nonlinear medium, was first developed by Bespalov and Talanov[1], and that theory has been verified experimentally by Bliss et al.[2] Trenholme[3] has extended the Bespalov-Talanov analysis to the more complex case of a periodic array of nonamplifying glass slabs separated by air gaps. His results indicate that the simple Bespalov-Talanov theory for a single nonlinear medium will not accurately predict certain features of ripple amplification in more complicated amplifier systems.

Ripple gain in the CYCLOPS laser system has been under experimental study by Bliss. The current work is intended to provide insight into these experiments and to provide an efficient and general calculational tool for studying ripple gain in complex, realistic laser amplifier systems, including beam divergence. The importance of beam divergence is two-fold: first of all it magnifies ripple wavelengths, and, secondly, it changes effective air spacings between elements and thus effectively removes periodicities that might otherwise exist for a collimated beam.

The FLAC Code

The FLAC (Fourier Laser Amplifier Code) is a general purpose three-dimensional (x,y,z-dependent) nonlinear optics code that is based on a

finite Fourier series solution of Maxwell's wave equation in Fresnel approximation.[4] It can be shown that the accuracy of this solution method is limited only by the ability of the calculational mesh to resolve the relevant Fourier components in a given problem. The method is very fast when implemented with the fast Fourier transform (FFT) algorithm. For reasons of both computational speed and numerical accuracy the finite Fourier series method of solution is highly efficient.

The maximum size transverse mesh the code can employ is 128 x 128. If the problem has inversion symmetry with respect to the x and y-axis, the code can utilize cosine transforms, and calculation is required in only the upper right-hand quadrant of the transverse plane. This increases the effective beam resolution by a factor of 2 and the effective number of mesh points by a factor of 4.

The code has been written to handle an arbitrary number of system elements in sequence. Disc modules are specified by number of discs, air gap spacing, and disc thickness. Propagation through air requires calculation of a single Fourier and inverse Fourier transform pair. Propagation through nonlinear elements requires the phase to be updated in segmented steps along the axial (z) direction. The presence of lenses is treated by a lens transformation consisting of a suitable rescaling of the z-coordinate and the transverse grid. Propagation through a spatial filter requires calculation of a Fourier transform, a filtering operation, followed by an inverse Fourier transform. The effect of refraction at a disc interface is modeled by stretching the computational mesh along the principle disc axis. When the laser beam passes through a Faraday rotator in the amplifier chain,

the direction of polarization and the orientation of the principle axis of the disc module are rotated by 45°. This creates a nonrectangular distortion in the computational mesh inside a tilted disc. This distortion cannot be treated by the code in its present form. The effect of crossing two Faraday rotators, however, will result in a total rotation of the polarization vector and disc orientation by 90°. This orientational change can be treated. This suggests that 45° rotations be ignored but that after every pair of Faraday rotators the code should take into account the rotation of the disc orientations by 90°.

The FLAC code was originally designed for the same number of grid lines in both the x and the y-direction. It has recently been rewritten to apply to a general mesh whose numerical dimensions must only be some power of 2. This general mesh capability has a bearing on the efficiency of ripple gain spectrum calculations. (See the following section.)

Application of the FLAC Code to Ripple Gain Calculations

To generalize the results of Bespalov and Talanov[1], one needs to propagate a beam with the initial form

$$E = E_0(1 + \varepsilon e^{i(k_x x + k_y y)}) \, e^{i\alpha(x^2+y^2)} \qquad (1)$$

through the entire amplifier chain. Here E_0 is the magnitude of the background field, ε is a complex plane-wave perturbed amplitude, and α is a measure of the initial beam divergence. It can be shown in the linearized approximation of the Fresnel equation that the perturbed wave uncouples in the x and y-directions. Hence, when a linearized treatment is valid, one need only consider beams of form

$$E = E_0(1 + \varepsilon e^{ikx}) \, e^{i\alpha(x^2+y^2)} \qquad . \qquad (2)$$

The phase factor can be removed with a lens transformation, and the problem becomes one-dimensional. One could in principle run a host of calculations for a range of k-values to determine $|\varepsilon(z=z_{max})|/|\varepsilon(z=0)|$ as a function of k. It is much more efficient, however, to make use of the spectral basis of the code. One propagates instead the beam

$$E = E_0(1 + \varepsilon\delta(x)) \quad . \tag{3}$$

The δ-function can be represented as

$$\delta(x) \sim \sum_k e^{ikx} \quad , \tag{4}$$

which contains all of the Fourier components that can be realized on the computational mesh, with equal amplitudes. By analyzing the spectral output at the end of the amplifier chain, one obtains the entire Bespalov-Talanov gain spectrum from a single run. By running several calculations with differing transverse mesh spacings (Δx values) one can span a logarithmic range in k.

To compute the maximum ripple gain for each value of k, one calculates the ripple gain spectra for the two perturbations $E_1 = E_0\varepsilon\delta(x)$ and $E_2 = E_0 i\varepsilon\delta(x)$, where E_0 is real. One then determines the phase angle $\theta(k)$ that makes the gain of $(\cos\theta + i \sin\theta)\ \varepsilon \cos kx$ a maximum. Due to the assumed linearity of the problem this can be done using the results of the two propagation calculations with E_1 and E_2 as assumed perturbations. One thus obtains the maximum ripple gain that can be encountered for any value of x by an appropriate combination of amplitude and phase perturbations. Naturally the input number ε must be small enough to insure that the linearized value of k for an appropriate approximation is valid, but large enough to make round-off error unimportant.

Numerical Results for CYCLOPS Laser System

The FLAC code has been used to simulate the CYCLOPS laser system up to the third B-module and to calculate the maximum ripple gain spectrum, $\max\{\ell n|E(k, \text{3rd B-module})/E(k,0)|\}$. Our model of this portion of CYLCOPS consists of 33 segments that correspond to 20 optical elements (simulation of the pocket cell requires 2 segments and 12 external air spaces. Disc modules also contain air spaces but are counted as single elements. See Figure 1.

When the laser beam enters the Brewster angle slabs of the the 2 single and 3 double plate polarizers and the 5 disc amplifiers, FLAC automatically accounts for the decrease of the intensity by the factor 1/n and the increase of the ripple wavelength by the factor n for ripple wave vectors in the plane of incidence. For the purposes of these initial simulations, the ripple wavevector was taken to be in the plane of incidence although a more correct model would rotate the plane of incidence 90° for each pair of Faraday rotators that the laser beam passes through. The small signal gain of the rod and disc amplifiers, the simple n_2 non-linearity and surface losses of the glass and crystal elements, and the divergence of the laser beam (including the effect of lenses between the A and B modules) were all included in the calculations.

By using a lens transformation to remove the quadratic phase front, the y dependence of the calculation is removed and the unperturbed spherical wave becomes the $k_x = 0$ Fourier component; then in the linearized approximation each of the non-zero k_x Fourier components grows independently and gives a point of the ripple gain spectrum.

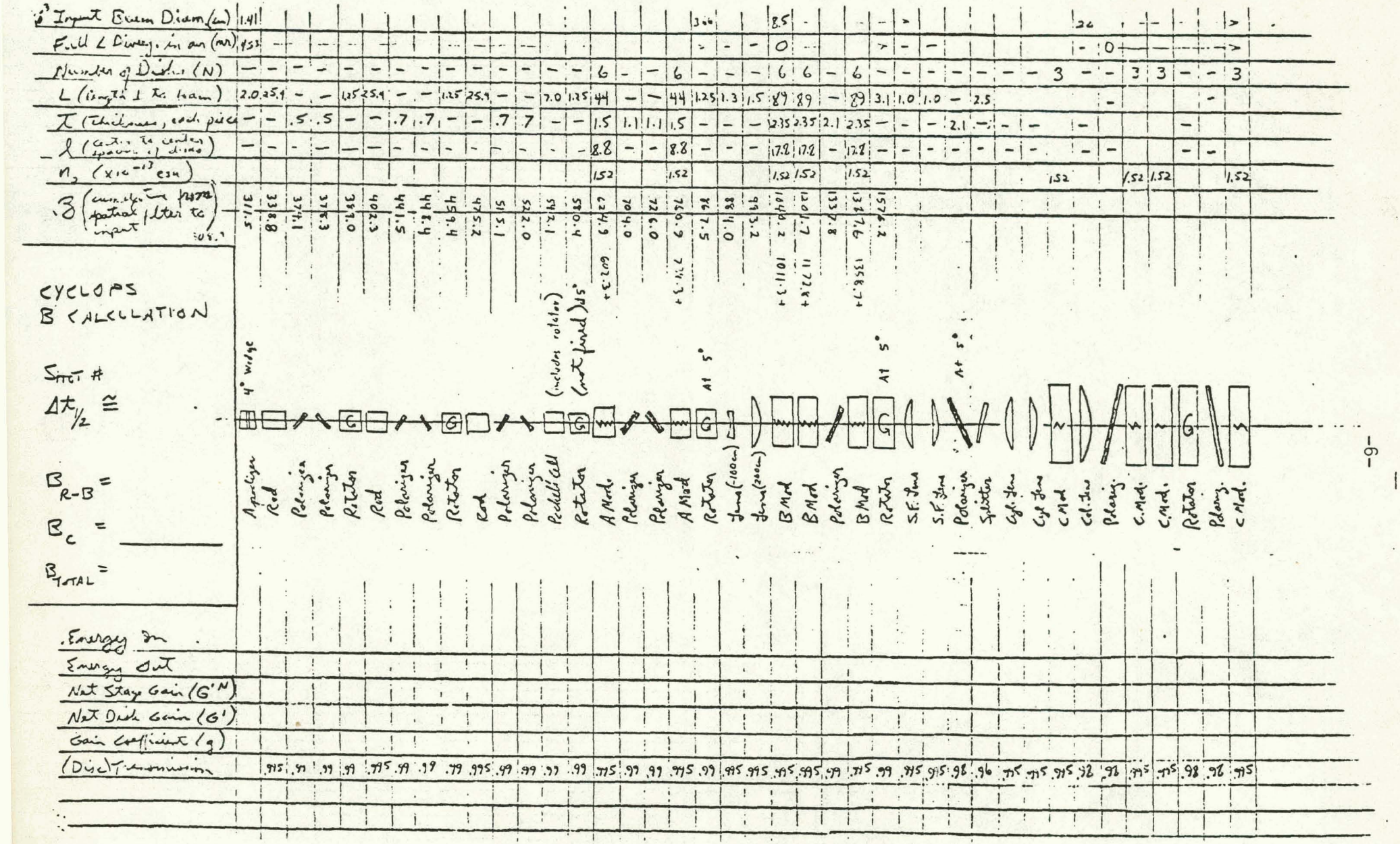
Input Beam Diam (cm)
Full ∠ Divergence in air (mr)
Number of Disks (N)
L (length ⊥ to beam)
t (Thickness, each piece)
ℓ (center to center spacing of disks)
n₂ (x10⁻⁶ esu)
β (cumulative phase shift to input)
CYCLOPS
B CALCULATION
Sheet #
Δt½ ≅
B R-B =
B C =
B TOTAL =
Energy In
Energy Out
Net Stage Gain (G'N)
Net Disk Gain (G')
Gain Coefficient (g)
(Disk) Transmission
4° wedge
(includes rotator)
(mostly fixed) 45°
At 5°
At 5°
At 5°
Aperture Rod
Polarizer
Polarizer
Rotator
Rod
Polarizer
Polarizer
Rotator
Rod
Polarizer
Polarizer
Pockels Cell
Rotator
A Mod.
Polarizer
Polarizer
A Mod
Rotator
Lens (-100cm)
Lens (200cm)
B Mod
B Mod
Polarizer
B Mod
Rotator
S.F. lens
S.F. lens
Polarizer
Spatial
Cyl. lens
Cyl. lens
C Mod
Cal. lens
Polariz.
C. Mod.
C Mod.
Rotator
Polariz.
C Mod.

FLAC was originally written as a two-transverse-dimensional code with an equal number of mesh points along the x and y axes. Since linearized ripple gain calculations can be done with one transverse dimension, FLAC has been recoded to allow the number of mesh points along the x and y axes to be independent of each other and to be any power of two between 4 and 128. With the old FLAC several 64 x 64 calculations requiring approximately 4.5 min each, were required to span the spatial frequency domain in which significant gain spectrum values exist. The same spectrum calculation can now be done with better resolution on the new FLAC with half as many 128 x 4 calculations requiring only 1.2 min each.

Over 45 FLAC calculations have been run in the course of this investigation. Checks were made on whether the z-step size and perturbation amplitude were small enough, and several runs with different input power levels were made. Some of these runs were used to check the generalization of the code's generalized mesh features. Most of the runs were used to check whether one could obtain the Bespalov-Talanov spectrum by analysing the spatial spectrum of the output beam for a single code run with a δ-function input. This was done by comparing the spectrum so obtained with a spectrum obtained by propagating each individual Fourier component separately. These calculations verified that a single propagation run could indeed yield the correct ripple spectrum.

Figure 2 is a low resolution maximum ripple gain spectrum of the CYCLOPS laser system for which the B integral was 3.94 and the cut-off spatial frequency was approximately 400 cm^{-1} at the output surface of the third B module. Although it is complicated by the amplifier gain, the beam divergence, and the many incommensurate spacings between glass elements, this spectrum is

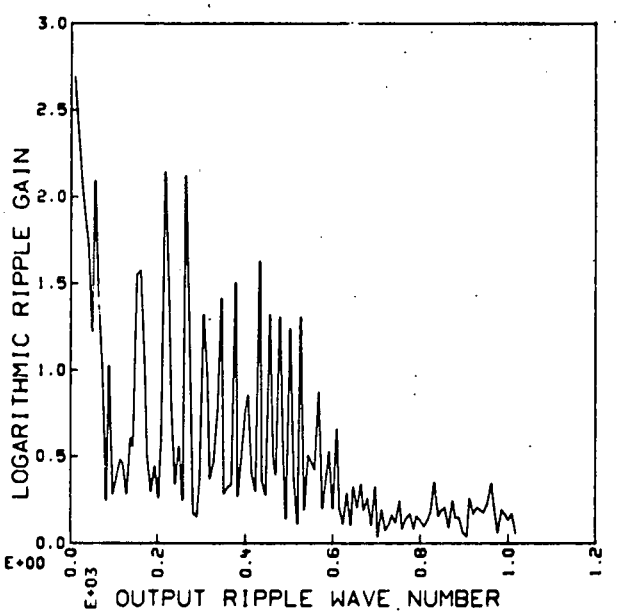

Figure 2. Maximum ripple gain spectrum for the CYCLOPS laser system through the third B-module for 11.5 GW/cm^2 output intensity.

similar to Trenholme's result for two identical glass slabs[3] in the following respects: both have a broad peak near zero spatial frequency followed by a series of peaks that become progressively narrower at higher spatial frequencies and that extend beyond the cut-off frequency for the output intensity. There is, however, one significant difference. The largest maximum ripple gain observable in the present results is less than 3, which compares with a B integral value of 3.94. For Trenholme's simpler calculation, on the other hand, the largest maximum ripple gain is still given by the B integral.

Figure 3 shows the spatial frequency part of Fig. 2 at higher resolution and shows spectral output intensities one-half and one-tenth of the value used in Fig. 2. For wavelengths shorter than 2.5 cm, Fig. 4 contains the same information as Fig. 3 plotted versus ripple wavelengths. Note that the peak around 1.2 mm corresponds roughly to the separation of hot spots in the near field intensity taken after the third B module in the CYCLOPS laser.[5]

Note added in proof

We have added the optical elements between the third B-module and the fourth C-module to our model of the CYCLOPS laser. This required 23 additional computational elements: seven Brewster angle disc stacks together with the air space that immediately follows each (four C-modules and three single-plate polarizers), a spatial filter, sever glass slabs (the two cylindrical lenses, the two Faraday rotators, the glass in the two spatial filter lenses, and the beam splitter), the collimating lens, and seven separately modeled air spaces.

These FLAC runs make use of a linearized analysis of the ripple gain, even though the experimental results[1] indicate a significant transfer of

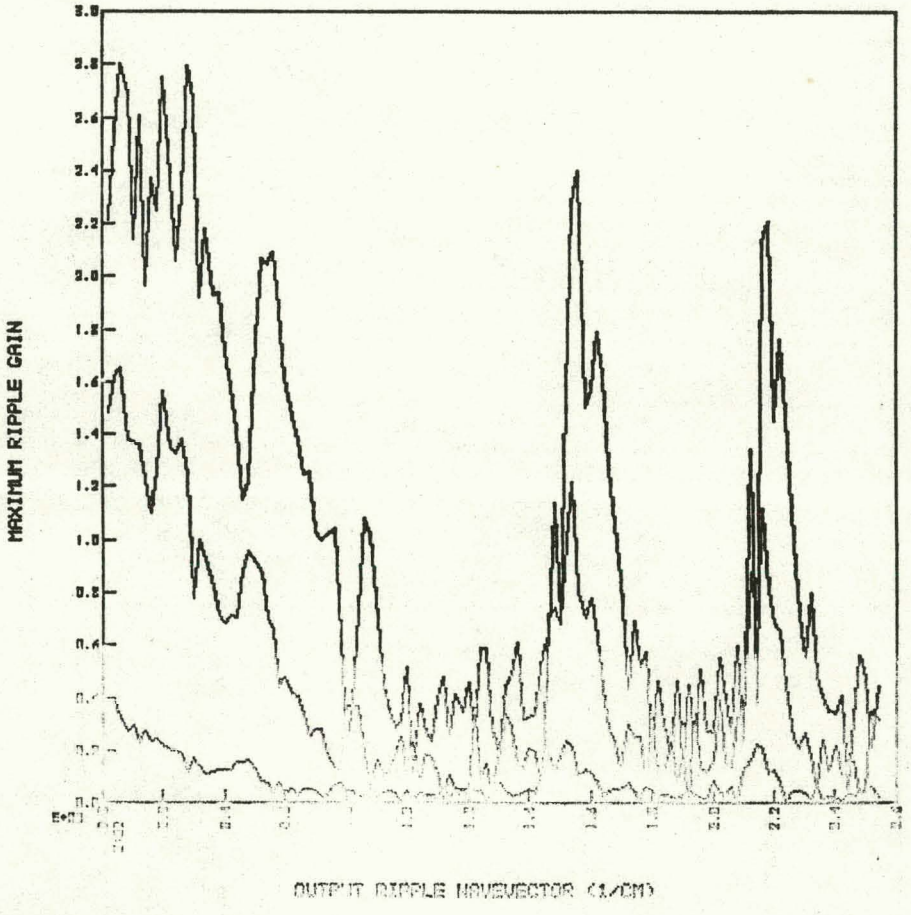

Figure 3. High resolution maximum ripple gain spectrum for wavevectors less than 250 cm^{-1} and for 11.5, 5.77, and 1.15 GW/cm^2 output intensities in the CYCLOPS laser system through the third B-module.

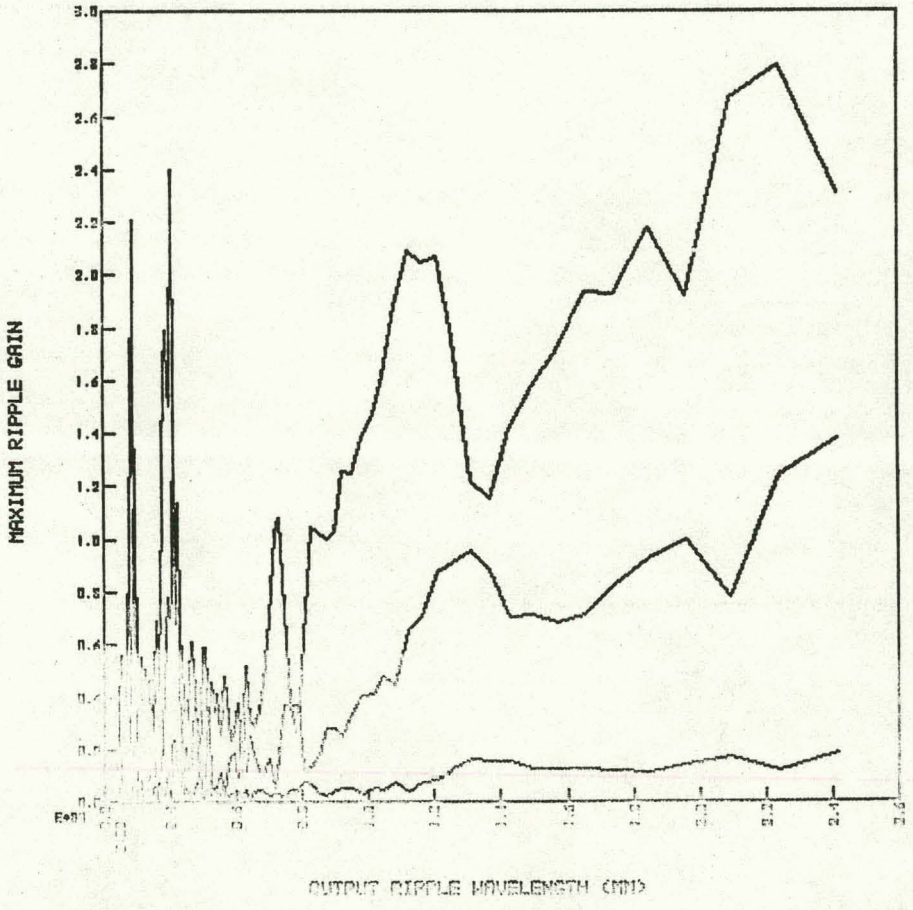

Figure 4. Maximum ripple gain versus the output ripple wavelengths for 11.5, 5.77, and 1.15 GW/cm^2 output intensities in the CYCLOPS laser system through the third B-module.

energy into ripple modes above the spatial filter cut-off spatial frequency. We have reduced the intensity uniformly for all Fourier components at the spatial filter output lens by the spatial filter loss factor, 17.5j/23.9j = .732. Although this correction is somewhat artificial, it has the desireable properties of giving the correct intensities after the spatial filter and making the ripple gain for unfiltered modes continuous through the spatial filter.

Figures 5 and 6 show the maximum ripple gain at the output face of the fourth C-module plotted as functions of the ripple spatial frequency and the ripple wavelength, respectively. The arrow along the abscissae of these plots is at the 3.88 cm^{-1} cut-off frequency (1.6 cm wavelength) of the spatial filter with its pinhole diameter of 300μ. Thus the spatial filter is seen to be quite effective in removing from the beam unwanted ripple noise. The cause of the relatively high gain in the long wave length portion of the spectrum is the large amount of beam divergence in the CYCLOPS system, which magnifies the small wave length of components that may be important in an early portion of the amplifier chain into long wavelengths at later stages.

The dominant features of the spectrum displayed in Figs. 3-6 are a very broad peak extending from 3.1 mm to greater than 2.0 cm ripple wavelengths and a narrower double peak between 2.0 and 2.7 mm. These features agree qualitatively with near field intensity data[5] taken after the fourth C-module in which hot spot separations for 2 mm up seem to dominate.

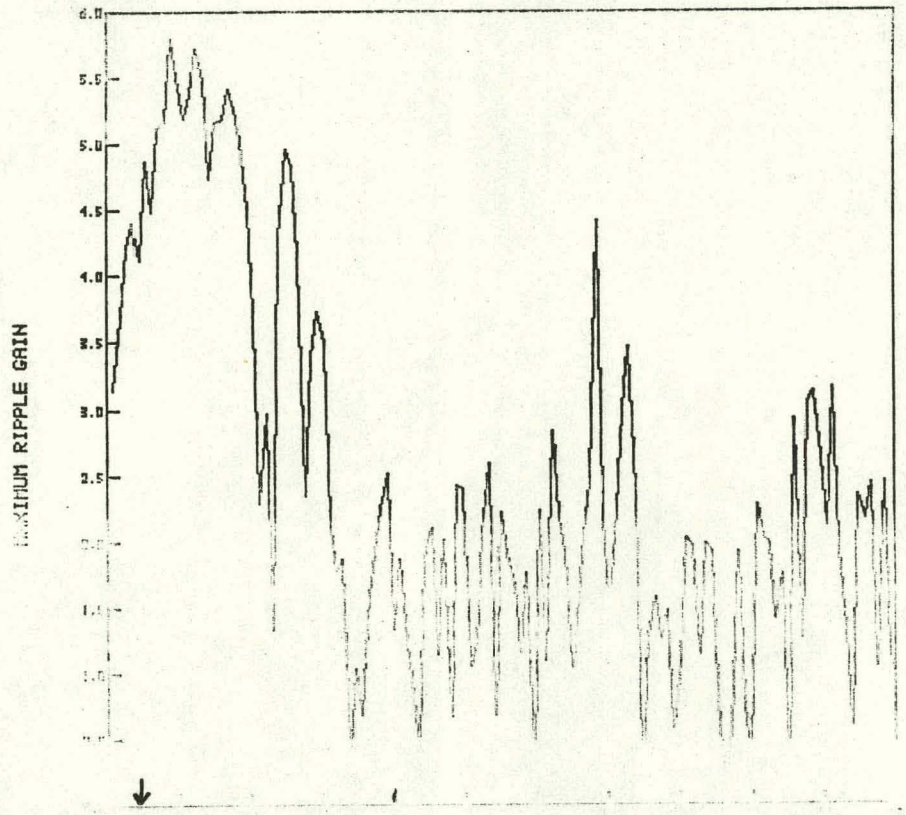

Figure 5. Maximum ripple gain for the CYCLOPS laser from the apodized aperture through the fourth C-module versus the output ripple spatial frequency for an output intensity of 8.2 GW/cm^2 and a B integral value of 9.2.

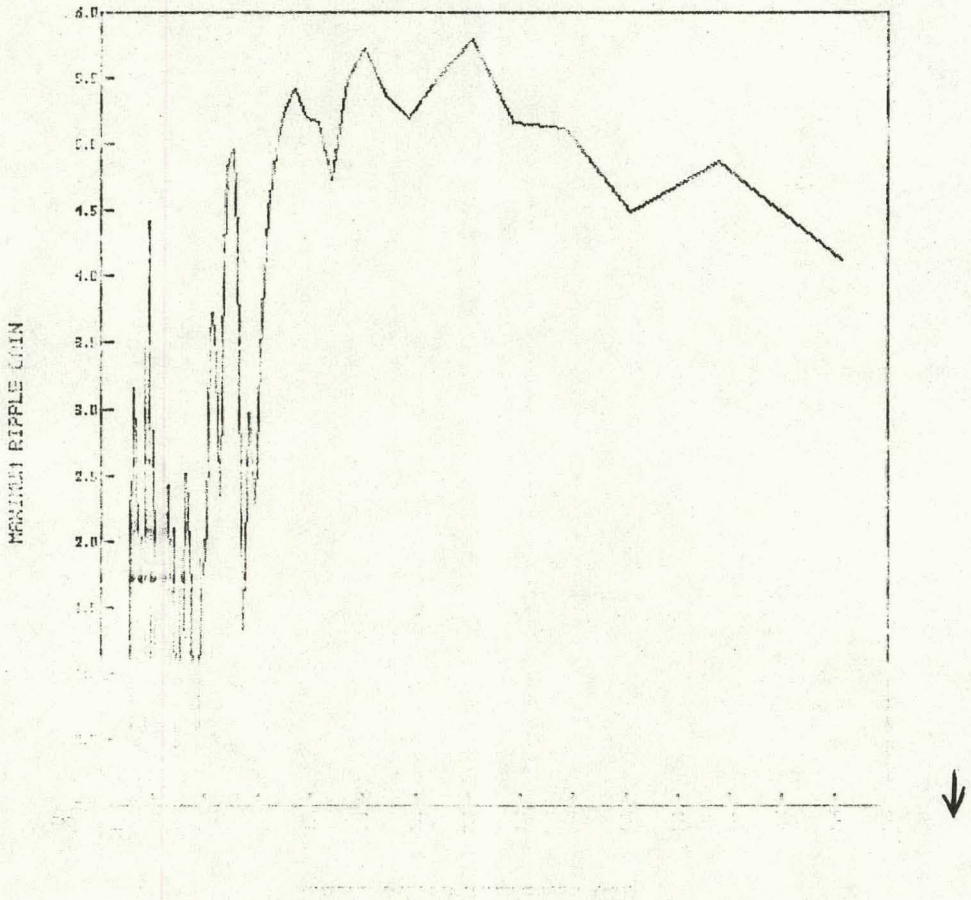

Figure 6. Same as fig. but versus ripple wavelength.

fig 6

References

1. U. I. Bespalov and V. I. Talanov, JETP Lett. 3, 307 (1966).

2. E. S. Bliss, D. R. Speck, J. F. Holzrichter, J. H. Erkkila, and A. J. Glass, Appl. Phys. Lett. 25, 448 (1974).

3. John Trenholme, Laser Program Annual Report - 1974, Lawrence Livermore Laboratory, Rept. UCRL-50021-74, p. 190.

4. J. A. Fleck, Jr., J. R. Morris, and M. D. Feit, "Time-Dependent Propagation of High Energy Laser Beams Through the Atmosphere I", Applied Physics 10, 129-160 (1976).

5. E. S. Bliss, private communication.

Distribution

Internal

Erlin Bliss
John Emmett
J. A. Fleck, Jr.
Alexander Glass
Jim Glaze
John Hunt
R. E. Kidder
J. R. Morris
John Trenholme
Bill Simmons
Tom Wainwright

T-Division (3)

T.I.D. (15)

T.I.C. (27)

External

Farres Mattar
University of Rochester
Laser Energetics Lab.
River Station Campus
Rochester, New York 14627

Printed in the United States of America
Available from
National Technical Information Service
U.S. Department of Commerce
5285 Port Royal Road
Springfield, VA 22161
Price: Printed Copy $; Microfiche $3.00

Page Range	Domestic Price	Page Range	Domestic Price
001–025	$ 3.50	326–350	10.00
026–050	4.00	351–375	10.50
051–075	4.50	376–400	10.75
076–100	5.00	401–425	11.00
101–125	5.50	426–450	11.75
126–150	6.00	451–475	12.00
151–175	6.75	476–500	12.50
176–200	7.50	501–525	12.75
201–225	7.75	526–550	13.00
226–250	8.00	551–575	13.50
251–275	9.00	576–600	13.75
276–300	9.25	601–up	*
301–325	9.75		

*Add $2.50 for each additional 100 page increment from 601 to 1,000 pages; add $4.50 for each additional 100 page increment over 1,000 pages.

Technical Information Department
LAWRENCE LIVERMORE LABORATORY
University of California | Livermore, California | 94550